AGU PUBLICATIONS

Geophysical Research Letters

RESEARCH LETTER
10.1002/2017GL075601

Key Points:
- Merging climate models and ice core data gives seasonality and spatial pattern of deglacial warming
- Temperature fields are useful for forcing ice sheet models and interpreting local ice retreat
- Temperature seasonality expedites deglacial ice loss and mutes the impact of abrupt climate change

Supporting Information:
- Supporting Information S1
- Data Set S1

Correspondence to:
C. Buizert,
buizertc@oregonstate.edu

Citation:
Buizert, C., Keisling, B. A., Box, J. E., He, F., Carlson, A. E., Sinclair, G., & DeConto, R. M. (2018). Greenland-wide seasonal temperatures during the last deglaciation. *Geophysical Research Letters*, *45*. https://doi.org/10.1002/2017GL075601

Received 7 SEP 2017
Accepted 31 JAN 2018
Accepted article online 7 FEB 2018

Greenland-Wide Seasonal Temperatures During the Last Deglaciation

C. Buizert[1], B. A. Keisling[2], J. E. Box[3], F. He[1,4], A. E. Carlson[1], G. Sinclair[1], and R. M. DeConto[2]

[1]College of Earth, Ocean, and Atmospheric Sciences, Oregon State University, Corvallis, OR, USA, [2]Department of Geosciences, University of Massachusetts Amherst, Amherst, MA, USA, [3]Geologic Survey of Denmark and Greenland (GEUS), Copenhagen, Denmark, [4]Center for Climatic Research, University of Wisconsin-Madison, Madison, WI, USA

Abstract The sensitivity of the Greenland ice sheet to climate forcing is of key importance in assessing its contribution to past and future sea level rise. Surface mass loss occurs during summer, and accounting for temperature seasonality is critical in simulating ice sheet evolution and in interpreting glacial landforms and chronologies. Ice core records constrain the timing and magnitude of climate change but are largely limited to annual mean estimates from the ice sheet interior. Here we merge ice core reconstructions with transient climate model simulations to generate Greenland-wide and seasonally resolved surface air temperature fields during the last deglaciation. Greenland summer temperatures peak in the early Holocene, consistent with records of ice core melt layers. We perform deglacial Greenland ice sheet model simulations to demonstrate that accounting for realistic temperature seasonality decreases simulated glacial ice volume, expedites the deglacial margin retreat, mutes the impact of abrupt climate warming, and gives rise to a clear Holocene ice volume minimum.

Plain Language Summary The Greenland ice sheet could contribute 7 m (23 feet) of sea level rise if it were to melt completely. For future sea level rise predictions we need to know how the Greenland ice sheet will respond to rising temperatures. We can figure out how sensitive Greenland is by studying a natural period of warming (called the last deglaciation) that happened at the end of the last Ice Age 18,000 years ago. During the last Ice Age the Greenland ice sheet was much larger than it is today, and as the climate warmed it shrunk to its present size. We combine ice core data and climate models to reconstruct Greenland-wide temperatures for all seasons over the last 22,000 years. This reconstruction makes it possible to simulate Greenland ice loss during the last deglaciation in ice sheet models. The model output can be compared to data on past ice sheet volume, for example, from moraines left behind in the landscape as the ice melted. Our reconstruction provides a critical step in learning from the past behavior of the Greenland ice sheet in order to predict its future.

1. Introduction

The sensitivity of the Greenland ice sheet (GIS) to climate change determines its contribution to past and future sea level rise. The past extent of the GIS has differed significantly from the present day. During the Last Glacial Maximum (LGM) from approximately 26 to 19 thousand years (ka) before present (BP, with present defined as the year 1950 Common Era), the ice sheet was much more extensive, growing out to the continental shelf break in most locations (Funder et al., 2011). In contrast, during the Holocene thermal maximum (HTM, 10–6 ka BP) it retreated to within its present margin (Bennike & Weidick, 2001; Briner et al., 2010, 2013, 2014; Carlson et al., 2014; Cronauer et al., 2016; Larsen et al., 2015; Young, Briner, Stewart, et al., 2011; Young & Briner, 2015). Burial dating of bedrock material recovered beneath the Greenland Ice Sheet Project-2 (GISP2) ice core indicates protracted deglaciated periods in central Greenland during the Pleistocene (Schaefer et al., 2016), suggesting a high sensitivity of the GIS to warming. Marine and ice cores provide evidence for the GIS response during the last interglacial period (a time period with a polar climate that is warmer than today), suggesting a smaller-than-present GIS that still covered much of the island (Colville et al., 2011; NEEM community members, 2013; Yau et al., 2016). Over the next decades, the GIS and its glaciers are projected to be the third largest contributor to global sea level rise—after thermal expansion and land-based glaciers (Intergovernmental Panel on Climate Change, 2013). Under sustained warming, Greenland has the potential

to contribute over 7 m of sea level rise, providing great impetus to better understand the stability and potential thresholds of the ice sheet (Clark et al., 2016; Robinson et al., 2012).

The last deglaciation (19–7 ka BP) presents a natural experiment in which to assess the sensitivity of the GIS. Its past extent is recorded in glacial landforms such as moraines (e.g., Denton et al., 2005; Funder et al., 2011; Kelly et al., 2008; Levy et al., 2016; Rinterknecht et al., 2014; Young, Briner, Axford, et al., 2011; Young et al., 2013) and most precisely reconstructed using exposure dating techniques (e.g., Carlson et al., 2014; Corbett et al., 2011; Hughes et al., 2012; Kelley et al., 2013; Larsen et al., 2014; Sinclair et al., 2016; Winsor et al., 2015; Young et al., 2013). Simultaneously, the (annual mean) temperature evolution can be reconstructed precisely from Greenland ice cores (Grootes et al., 1993; NGRIP community members, 2004; NEEM community members, 2013), allowing ice sheet modeling of the deglaciation in Greenland (Lecavalier et al., 2014; Simpson et al., 2009; Tarasov & Richard Peltier, 2002). The most accurate Greenland temperature reconstructions are based on $\delta^{15}N-N_2$, which is thermally fractionated in polar firn (Buizert et al., 2014; Kindler et al., 2014; Landais et al., 2004; Severinghaus et al., 1998). However, the $\delta^{15}N$ method provides mean annual temperatures, whereas GIS mass loss (at least in the present day) is concentrated in the summer season (Van den Broeke et al., 2009). Moreover, the ice core records are from interior Greenland, whereas the ice retreat occurs at the margins that may experience a different magnitude of warming.

Both for the purpose of forcing ice sheet models and for interpreting data on past Greenland ice margin positions, it is critical to have climate reconstructions that include temperature seasonality and that furthermore span the entire GIS. Coupled climate model simulations can, in principle, provide such information (Liu et al., 2009; Menviel et al., 2011), but they rely on somewhat arbitrary freshwater forcing scenarios, lack the spatial detail to resolve the steep topographic gradients of ice sheet ablation zones, and are not nearly as accurate as the ice core reconstructions. Here we merge the deglacial $\delta^{15}N$-based Greenland ice core reconstructions of Buizert et al. (2014) with the TraCE-21ka coupled ocean-atmosphere general circulation model (GCM) of the last deglaciation (Liu et al., 2009, 2012; He et al., 2013) to generate Greenland-wide, seasonally resolved deglacial temperature fields. In the merged product, the ice core record constrains the timing and magnitude of annual mean temperature evolution in central Greenland, and the climate model is used to infer the temperature seasonality and spatial pattern. To demonstrate the importance of accounting for temperature seasonality, we here perform and compare two deglacial ice sheet model simulations, which use either our estimated seasonality or a fixed, present-day seasonality.

2. Materials and Methods

2.1. Ice Core Reconstructions

Buizert et al. (2014) use an inverse modeling technique in which temperature and accumulation scenarios are obtained that optimize the fit of firn densification model simulations to both $\delta^{15}N$ data and (data-based) constraints on the ice core gas age-ice age difference (Δage). Reconstructions are available for the Greenland GISP2, North Greenland Ice Core Project (NGRIP) and North Greenland Eemian Ice Drilling (NEEM) ice cores for the 22–10 ka period. We have extended the GISP2 reconstruction through the Holocene using the same techniques—this Holocene extension is only possible for the GISP2 ice core where high-resolution $\delta^{15}N$ data exist (Kobashi et al., 2008). Mean annual temperatures around the 8.2 ka event are well constrained due to its clear Δage marker (Kobashi et al., 2007). Details on the reconstruction method can be found in the supporting information and in (Buizert et al., 2014). A compilation of GISP2 $\delta^{15}N$ data is given by Seierstad et al. (2014).

For the last 4,000 years we further make use of the GISP2 temperature reconstruction by Kobashi et al. (2011), which is based on combining $\delta^{15}N$ and $\delta^{40}Ar$ data. For the period 1840 to present the reconstructions by Box et al. (2009, 2013) are used.

2.2. Transient Climate Model Simulations

We use transient, nonaccelerated climate model simulations for the last 22 ka (TraCE-21ka) using the Community Climate System Model version 3 (CCSM3) coupled ocean-atmosphere GCM (Liu et al., 2009, 2012; He et al., 2013). Ice sheet elevations are prescribed following ICE-5G (Peltier, 2004), greenhouse gas concentrations follow Monnin et al. (2001), and variations in the Atlantic Meridional Overturning Circulation (AMOC) are induced using freshwater forcing in the North Atlantic and elsewhere, with freshwater scenarios based on Carlson and Clark (2012). Model output is available at monthly time resolution and T31 grid (approximately 3.75° resolution).

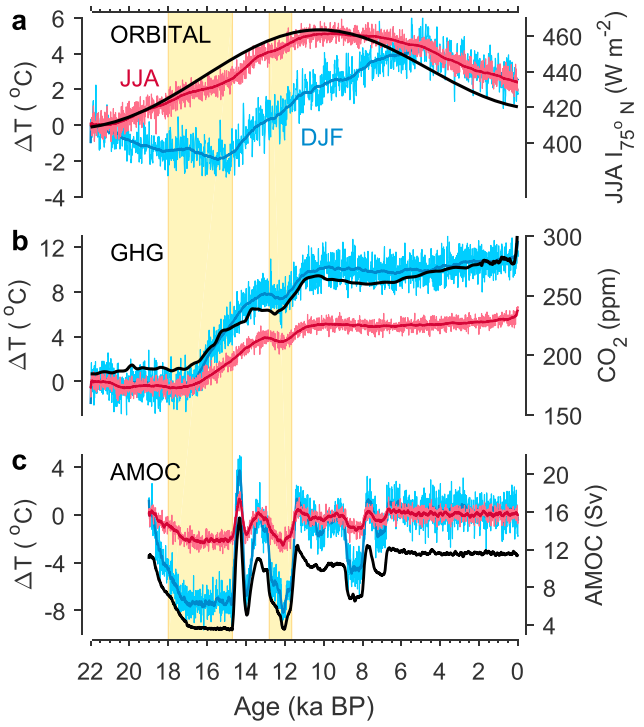

Figure 1. Greenland summer (June–August (JJA), red curves) and winter (December–February (DJF), blue curves) temperatures (left axes) in the TraCE-21Ka single forcing simulations (He et al., 2013). (a) Response to orbital forcing, with in black (right axis) the JJA mean insolation at 75°N. (b) Response to greenhouse gas forcing, with in black (right axis) the CO_2 forcing from Monnin et al. (2001) used in the TraCE simulations; the European Project for Ice Coring in Antarctica Dome C ice core time scale used has since been updated, which is not reflected in the simulations. (c) Response to freshwater forcing, with in black (right axis) the TraCE-simulated Atlantic Meridional Overturning Circulation (AMOC) strength in sverdrup (Sv) (10^6 m^3 s^{-1}). Seasonal temperatures are averaged over the GISP2, NGRIP and NEEM coring locations and shown as anomalies relative to 22 ka before present (start of simulations).

In addition to the full simulations, we use TraCE-21Ka single-forcing simulations in which the orbital, greenhouse gas, or freshwater (i.e., AMOC) forcing is applied, with the other forcings held fixed at 22 ka levels (He et al., 2013); these simulations provide valuable insight into how the various forcings affect seasonality (section 3.1).

2.3. Present-Day Climatology

Present-day Greenland temperature is based on the monthly reconstruction by Box et al. (2009), combining meteorological station records and regional climate model output; snow accumulation rates (also needed for the ice sheet model simulations) are based on Box (2013) and Box et al. (2013). We extend the reconstructions by Box et al. (2009) and Box (2013) through 2014 using the same methodologies. Temperatures for the period 1981–2010 are averaged to construct the monthly mean reference climatology; the data-model merged product presented here is expressed relative to this baseline. For the period 1840 to present our temperature fields will follow those of Box et al. (2009). The Box et al. (2009) reconstruction has a spatial resolution better than 0.5° longitude and better than 0.05° latitude.

2.4. Data-Model Merged Temperatures

Our deglacial temperature fields give decadal-average monthly temperatures from 22 ka BP to 2010 Common Era. The domain is from 96° to 0°W at 0.5° resolution and from 58° to 85°N at 0.25° resolution. The domain was selected to include all of the GIS, the surrounding continental shelf, and most of the Canadian Arctic Archipelago to allow an Innuitian Ice Sheet in ice sheet model simulations, which can influence the GIS via an ice saddle across Nares Strait or an ice shelf over Baffin Bay. Details on how the above mentioned products were merged into a single temperature field are described in section 3.2.

2.5. Ice Sheet Modeling

We run a three-dimensional thermomechanical hybrid ice sheet model at 10 km horizontal resolution, as documented elsewhere (DeConto & Pollard, 2016; Pollard & DeConto, 2012; Pollard et al., 2015). The model is spun up under LGM (21 ka) boundary conditions for 40,000 years. Climate forcing is applied on a 40 × 40 km grid and downscaled to the 10 km model grid using lapse rates (that correct for the different elevations in the coarse and fine grids) for temperature (5°C km^{-1}) (linear, Abe-Ouchi et al., 2007) and precipitation (10°C per doubling of precipitation) (exponential, Ritz et al., 2001). Those same lapse rates are used to correct for surface elevation differences between the simulated ice sheet and the reference ice sheet digital elevation model on which the climate forcings are defined. Surface mass balance is calculated using a positive degree-day scheme with 1 month time step; fresh snow is ablated first (at rate of 0.005 m $°C^{-1}$ d^{-1}), followed by bare ice (0.008 m $°C^{-1}$ d^{-1}). Following a refreezing correction, rain and meltwater are treated as runoff and immediately removed. Ocean melt rates are calculated for all nongrounded grid points and are proportional to the squared difference between the local ocean temperature and the freezing point of seawater at the ice depth (Martin et al., 2011; Pollard & DeConto, 2012). Ice flow is captured by heuristic scaling of the two relevant physical approximations to ice flow for "shallow ice" and "shallow shelves." Grounding line position (and thereby ice extent) is a calculated rather than prescribed quantity in our model and evolves freely as atmospheric and oceanic changes drive ice sheet advance and retreat.

3. Results and Discussion

3.1. Temperature Seasonality of Climate Forcings

Changes in temperature seasonality are not available directly from the ice core record, so we rely on the climate model simulations. To explore the influence of various climate forcings on temperature seasonality, we turn to the single-forcing simulations (section 2.2). Simulated summer (June–August, JJA) and winter (December–February, DJF) surface air temperatures (SAT) are shown for the three most important forcings (Figure 1). Orbitally driven summer SAT peaks around 10 ka BP, following local insolation. Greenhouse gas

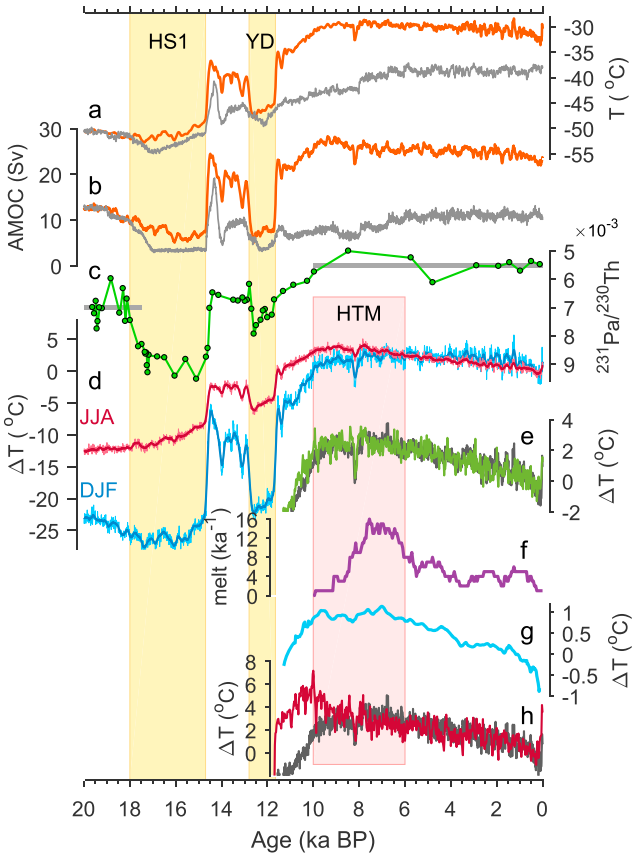

Figure 2. Atlantic Meridional Overturning Circulation (AMOC) and Greenland temperature. (a) TraCE-21Ka (Liu et al., 2009, 2012; He et al., 2013) simulated (gray) and reconstructed (orange) central Greenland temperature (based on average of GISP2, NGRIP and NEEM Ice Drilling locations for 22–10 ka, and GISP2 only for 10–0 ka before present, BP). (b) TraCE-21Ka simulated AMOC strength (gray) and AMOC strength required to bring TraCE-21 K simulations and ice core reconstructions into agreement (orange). (c) Bermuda rise ^{231}Pa/^{230}Th ratios as a proxy for AMOC strength (McManus et al., 2004). Horizontal bars denote data averages during the Last Glacial Maximum (22–18 ka BP) and "stable" part of the Holocene (10–0 ka BP). (d) Central Greenland summer (June–August, JJA, red) and winter (December–February, DJF, blue) temperatures relative to present in the data-model merged product. (e) Greenland Holocene temperature reconstruction (green curve) by (Vinther et al., 2009) and our merged product (gray curve) at the sites used (Renland and Agassiz). (f) GISP2 ice core melt record in number of melt layers per 1,000 years (Alley & Anandakrishnan, 1995). (g) Northern Hemisphere 30°N–90°N multiproxy temperature stack from Marcott et al. (2013). (h) Ellesmere Island temperature reconstruction (red curve) by Lecavalier et al. (2017) and our merged product (gray curve) at that site. Yellow bars denote Heinrich Stadial 1 (HS1) and the Younger Dryas (YD); red bar denotes the Holocene thermal maximum (HTM).

forcing warms DJF SAT by roughly twice as much as JJA SAT; the larger wintertime response to radiative forcing is in line with theory and modern observations (Intergovernmental Panel on Climate Change, 2013; Mitchell, 1989). Last, AMOC variations affect all seasons, but the response is strongest during the winter months due to amplification by sea ice extent (Fluckiger et al., 2008; Li et al., 2005). The single-forcing simulations are shown here for illustrative purposes; our temperature fields are based on the full model simulations in which all climate forcings are applied simultaneously.

3.2. Merging Models and Ice Cores

Figure 2a compares the ice core reconstruction of annual mean Greenland temperature (orange line, average of GISP2, NGRIP, and NEEM) with the TraCE-21Ka simulation (gray line, same locations). The simulation captures the Bølling abrupt transition (14.6 ka) fairly well, yet it fails to simulate the AMOC resumption (Figure 2b) and associated warming at the onset of the Holocene (11.7 ka BP). An alternative simulation in which the Bering Strait is kept closed does show a recovery of the AMOC at the Holocene onset and the associated warming (not shown). The failure of the model to simulate the Holocene onset (Figure 2a) is therefore due to its inability to resume a vigorous AMOC despite the need to still melt about the remaining Laurentide Ice Sheet (about half of its LGM size) into the North Atlantic and Arctic Oceans in the Holocene (Carlson & Clark, 2012; Ullman et al., 2016). The CCSM3 model used is likely overly sensitive to North Atlantic freshwater forcing and incorrectly biased toward monostability (Liu et al., 2015). Compared to the simulated AMOC variations, the orbital and greenhouse gas forcings are very well known from celestial mechanics and ice cores, respectively.

Based on the observations above, we make the following key assumption: we assume that the TraCE simulations correctly capture the Greenland climate response to increased greenhouse gas concentrations and orbital variations and that the model-data mismatch of Figure 2a is due solely to incorrectly simulated AMOC strength. We apply an AMOC correction to the model simulations in order to eliminate the model-data mismatch. This approach is in line with the observation of He et al. (2013), who show that the full deglacial climate simulation over Greenland (Figure 2a) is well approximated by the sum of the single-forcing simulations. The merged GIS temperature fields $T_{GIS}(\phi, \lambda, m, t)$, with latitude ϕ, longitude λ, month m and age t, are produced in the following way (with additional details given in the supporting information):

1. We determine the offset between the three-site average ice core temperature reconstruction $T_{IC}(t)$ (section 2.1) and (mean annual) model simulation $T_{GCM}(t)$ (section 2.2) at the same location(s).
2. We use the GCM simulations to determine the sensitivity $\alpha(\phi, \lambda, m)$ of local temperature to AMOC variability. We establish α in two ways, namely, (i) by dividing the magnitude of the Bølling warming by the associated AMOC increase and (ii) from linear regression of local temperature to AMOC strength in the AMOC-only single-forcing simulation. Both methods give similar results (Figure S5; at GISP2 the two methods give $\alpha = 0.81$ K Sv^{-1} and $\alpha = 0.89$ K Sv^{-1}, respectively), and we average the α values from these two methods for further use.
3. We determine the implied AMOC deficiency of the model as $\Delta\text{AMOC}(t) = \left[T_{IC}(t) - T_{GCM}(t)\right] / \alpha$, where we use the mean annual α value at the ice core locations. The simulated AMOC is shown in Figure 2b in gray, together with the implied AMOC in orange (simulated AMOC plus ΔAMOC). The implied AMOC strength for the present day is around 22 sverdrup (Sv), which is slightly more than current estimates of around 19 Sv (Talley, 2013).

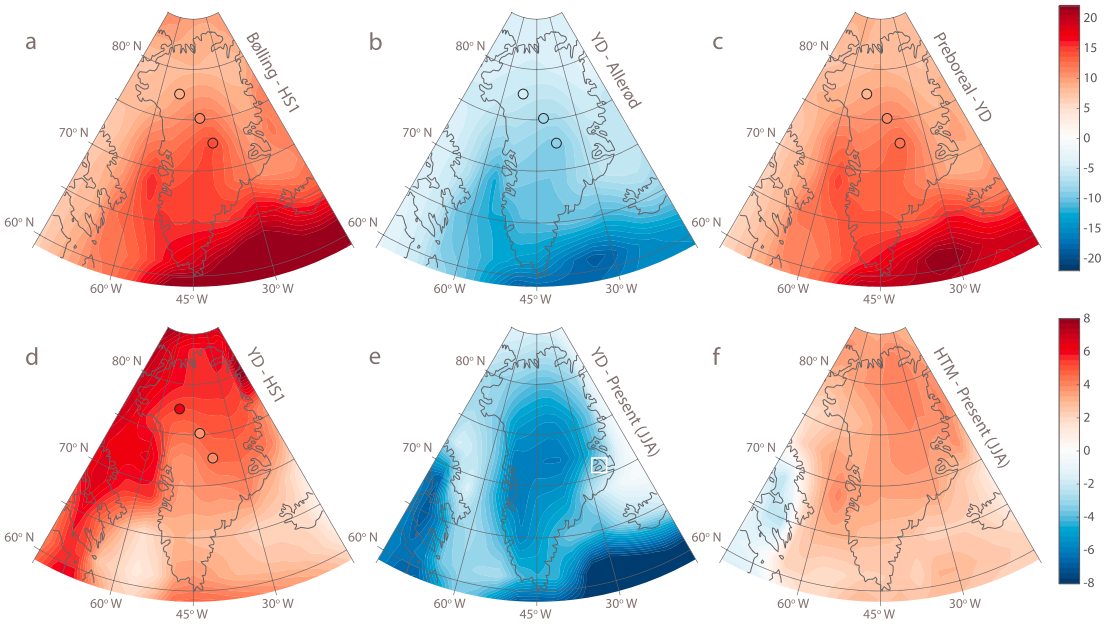

Figure 3. Deglacial Greenland temperature evolution. (a) The magnitude (annual mean) of the abrupt Bølling transition at 14.7 ka (Bølling minus HS1) in the merged product (color map) and in three ice cores (from north to south: NEEM, NGRIP and GISP2). (b) Same for Younger Dryas (YD) cooling at 12.8 ka (YD minus Allerød). (c) Same for Preboreal transition at 11.6 ka (Preboreal minus YD). (d) Same for YD minus HS1. (e) YD summer (June–August) temperatures relative to present. The Scoresby Sund study area of Denton et al. (2005) and Kelly et al. (2008) is marked by the white square. (f) Holocene thermal maximum (HTM) summer (June–August) temperatures relative to present. Figures 3a–3c use upper scale bar, Figures 3d–3f use lower scale bar, and color bar units are in degrees Celsius (°C).

4. We determine the temperature evolution for each month and at each location as $\Delta T(\phi, \lambda, m, t) = T_{\mathrm{GCM}}(\phi, \lambda, m, t) + \alpha(\phi, \lambda, m) \times \Delta\mathrm{AMOC}(t)$ (Figure 2d).
5. We ensure to match modern-day Greenland climatology by correcting for any potential offsets: $T_{\mathrm{GIS}}(\phi, \lambda, m, t) = \Delta T(\phi, \lambda, m, t) - C(\phi, \lambda, m)$ with correction C being the difference between ΔT and the Box et al. (2009) reconstruction for the 1981–2010 reference period.

3.3. Evaluating the GIS Surface Temperature Fields

First, we investigate whether our temperature fields agree with independent constraints and reconstructions. Our fields show an HTM from around 10–6 ka BP, which is most pronounced in summer (Figure 2d). Peak warmth slightly lags maximum summer insolation (Figure 1a) and is seen throughout Greenland with the largest magnitude in the northeast (Figure 3f). Figure 2e shows the Greenland Holocene (annual mean) temperature reconstruction by Vinther et al. (2009) in green, with our merged product (sampled at the same locations) in gray. We find an excellent agreement in both the timing and magnitude of temperature change—note that the data in Vinther et al. (2009) are not used in our work and that both records are therefore fully independent. Figure 2f shows the prevalence of melt layers in the GISP2 core, a proxy for local summer temperature (Alley & Anandakrishnan, 1995; Koerner & Fisher, 1990). The GISP2 melt layers suggest a summer thermal maximum from roughly 9–6 ka BP, shorter in duration than, but overlapping in time with, the broad HTM that we find in Greenland SAT between 10 and 6 ka BP (Figure 2d). Our HTM timing further agrees well with multiproxy reconstructions of Northern Hemisphere temperature (Figure 2g). Recently, Lecavalier et al. (2017) suggested that the timing of the HTM is earlier (11–10 ka BP) on Ellesmere Island, based on elevation-corrected records of summer melt and water isotopes—at that same location our merged product suggests maximum HTM warmth to occur around 9.5 ka BP (Figure 2h). The early warmth in the Lecavalier et al. (2017) reconstruction may be an high-latitude effect (Briner et al., 2016) not captured in the TraCE model simulation, a regional effect (such as the opening of Nares Strait (Zreda et al., 1999) or the demise of the Innuitian Ice Sheet (England et al., 2006)) or uncertainties in the model-based elevation correction used in the reconstruction (Lecavalier et al., 2013, 2017; Simon et al., 2015).

Our data-model merged product suggests HTM summer temperatures over Greenland are roughly 3.3°C above modern day—lower than melt-based reconstructions from Ellesmere Island (Lecavalier et al., 2017) of more than 5°C but in good agreement with the HTM reconstruction by Briner et al. (2016) of 3 ± 1°C.

In mean annual temperatures the HTM is less pronounced with around 2.1°C of warming. Our estimated HTM magnitude is about twice the Northern Hemisphere extratropical (30°–90°N) multiproxy average of ~1°C, as expected from polar amplification (Marcott et al., 2013).

An east Greenland valley glacier moraine sequence in the Scoresby Sund area suggests a Younger Dryas (YD) summer time cooling of only 4–6 °C relative to present (Broecker, 2006; Denton et al., 2005; Kelly et al., 2008; Levy et al., 2016), much smaller than the mean annual cooling of around 15°C (Severinghaus et al., 1998). These estimates are in good agreement with our merged product, which suggests about 4.4°C JJA cooling during the YD at Scoresby Sund (Figure 3e, white square). The only other YD-age moraines are found in Disko Bugt, confirming a still stand of the ice margin in west Greenland during the YD (Rinterknecht et al., 2014). The lack of YD moraines elsewhere on Greenland likely reflects that the ice sheet margin was still on the continental shelf in most regions during the YD (Briner et al., 2013; Dyke et al., 2014; Hughes et al., 2012; Kelley et al., 2013; Larsen et al., 2014; Sinclair et al., 2016; Winsor et al., 2015, 2015; Young et al., 2013).

Second, we investigate whether T_{GIS} matches the spatial patterns seen in the ice core reconstructions. Note that while T_{GIS} matches the three-site average T_{IC} by design, in our approach any gradients between the three cores are set by the GCM simulations. Figures 3a–3c show comparisons for the three abrupt transitions of the last deglaciation. For each transition both the ice cores and the merged product show amplified climate change upon going south—a fingerprint of the AMOC variations that induce the transitions (Buizert et al., 2014; Guillevic et al., 2013). Averaging over the three transitions, the ice cores suggest that at GISP2, NGRIP, and NEEM, the magnitude is respectively 1.23 ± 0.05, 1.03 ± 0.07, and 0.74 ± 0.08 times the average value (with 1σ spread between events). The merged temperature product gives relative magnitudes of 1.21 ± 0.03, 1.00 ± 0.01, and 0.79 ± 0.04, respectively. The spatial gradients during abrupt events thus agree well within the uncertainty bounds.

The warming between Heinrich Stadial 1 (HS1, or Oldest Dryas) and the YD has received attention in the literature due to the anomalous behavior of Greenland ice core $\delta^{18}O$ (Liu et al., 2012; Pausata & Löfverström, 2015). The spatial gradient in this warming trend (Figure 3d) is of the correct sign in the merged product, although it appears that the magnitude of the gradient is underestimated. The single-forcing simulations show the spatial gradient reflects retreat of the Laurentide Ice Sheet (Buizert et al., 2014). We speculate that the orographic effect of the ICE-5G reconstruction may be at fault, as this reconstruction is much larger than any other Laurentide Ice Sheet reconstruction (Carlson & Clark, 2012). Alternatively, ice dynamics may have altered T_{IC} or the relatively low spatial resolution of the climate model could be responsible.

Overall, we conclude that the merged, seasonally resolved temperature fields presented here for the last deglaciation provide a satisfactory fit to the sparse data constraints that are available. Improvements to the reconstruction would require more sophisticated and higher-resolution transient climate model simulations, additional ice core data from either existing or new cores, and ice core melt records from more locations and over longer time periods. At the time of writing the TraCE runs are the only available transient deglacial climate simulations using a fully coupled GCM. More such simulations are expected in the near future through the Paleoclimate Modelling Intercomparison Project framework (Ivanovic et al., 2016), which will allow for an improved evaluation of Greenland deglacial climate evolution.

The new merged temperature fields answer a lingering question of the apparent absence of a Greenland warming response to the deglacial CO_2 rise starting around 17.8 ka BP (Marcott et al., 2014). We find that the CO_2-driven warming competes with a cooling driven by a reduction in AMOC strength around the same time. The AMOC reduction influences the DJF temperature strongly, causing a net cooling during HS1 (Figure 2d). JJA temperature is much less sensitive to AMOC variability, and hence, summer warming is seen throughout HS1 in response to rising CO_2 and insolation.

3.4. Ice Sheet Modeling Results

Here we assess the influence of temperature seasonality on ice sheet model simulations of the last deglaciation. We force an ice sheet model (section 2.5) with (1) our seasonally resolved merged temperature fields as described above and (2) an alternative forcing that is identical to our data-model merged product in annual mean temperatures but preserves modern-day seasonality throughout (i.e., temperatures for each month vary together with the annual mean value). We shall refer to these as the VAR (variable) and FIX (fixed) seasonality forcings, respectively. Note that the FIX approach has been used in previous studies (e.g., Lecavalier et al., 2014; Simpson et al., 2009). Snow accumulation rates are identical for both simulations and based on the

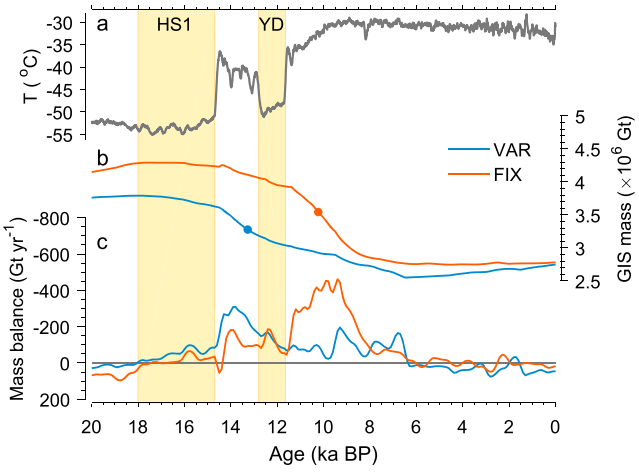

Figure 4. Simulations of Greenland ice sheet mass over the last 20 ka. (a) Greenland Summit mean annual temperature. (b) Total ice mass for simulations using variable seasonality (VAR, blue curve) and seasonality held at modern (FIX, red curve). Transition midpoints are marked as dots. (c) Total mass balance (Gt yr^{-1}) calculated by the ice sheet model using both forcings.

reference climatology (Box, 2013; Box et al., 2013) scaled linearly to reconstructed past accumulation rates from the GISP2 Summit ice core (Buizert et al., 2014; Cuffey & Clow, 1997). Figure 4 shows a comparison between the two simulations; maps of modeled ice sheet extent and thickness are in the supporting information (Figure S6).

The maximum simulated LGM GIS volume is 10.5 m (3.8×10^6 Gt) and 11.9 m (4.3×10^6 Gt) sea level equivalent volume for the VAR and FIX model runs, respectively. The larger FIX ice sheet is due to the colder summers in that forcing.

Temperature seasonality further has a large influence on the timing of ice sheet retreat. Overall, the use of realistic temperature seasonality expedites GIS retreat. We define the transition midpoint as the time at which the GIS reaches an ice mass midway between the simulated LGM and modern mass; these midpoints are marked as dots in Figure 4b. Using VAR forcing, the transition midpoint occurs around 3,000 years earlier than it does using FIX forcing.

It is well documented that GIS retreated to within its present-day margins in response to the HTM (Briner et al., 2013, 2014; Carlson et al., 2014; Cronauer et al., 2016; Larsen et al., 2015; Young, Briner, Stewart, et al., 2011; Young & Briner, 2015). Under VAR forcing a clear Holocene minimum in GIS mass is simulated around 6.5 ka BP of 2×10^5 Gt (0.55 m sea level equivalent) below present day. However, under FIX forcing the simulated ice sheet mass does not show a clear HTM minimum. The same problem was encountered by earlier studies using FIX-type forcing, who applied and ad hoc temperature correction to the ice core record to reproduce the GIS minimum (Lecavalier et al., 2014; Simpson et al., 2009). The HTM warmth is most pronounced in the summer months since it is driven by insolation. This HTM summer warming is captured in the VAR forcing but not in the FIX forcing, explaining the inability of the latter to drive significant GIS retreat.

Both forcings yield considerably increased mass loss in response to abrupt AMOC-forced warming. Under VAR forcing mass loss peaks in response to the Bølling warming (14.6 ka BP), and under FIX forcing in response to the Preboreal warming (11.6 ka BP). Maximum mass loss rates are about twice as large in the FIX scenario, because it has more summer warming than the VAR scenario and a larger ice sheet mass prior to the event. In general, using realistic temperature seasonality mutes the impact of the abrupt AMOC switches on ice sheet mass, because AMOC strength primarily impacts winter temperature (Figures 1c and 2d).

Besides the atmospheric forcing presented here, many additional factors control the GIS deglacial evolution—such factors include ocean temperatures, basal sediments and lubrication, and buttressing across Nares Strait. Future studies are needed to elucidate their relative importance and time evolution. A full assessment of ice sheet model skill would involve the fit to ^{14}C dates and ^{10}Be surface exposure ages (Dyke, 2004; Sinclair et al., 2016) and relative sea level records as a proxy for continental ice loading (Simpson et al., 2009); this is beyond the scope of the present work. The ice sheet model comparison shown here highlights the importance of seasonality in driving the ice sheet response to climate change. By providing a realistic, climate model-based estimate of temperature seasonality, the present work represents a step toward a higher degree of model realism in simulating the GIS through the last deglaciation.

4. Conclusions

We have merged Greenland ice core temperature reconstructions that constrain the timing and magnitude of annual mean climate change, with climate model simulations that constrain its seasonality and spatial pattern, to produce Greenland-wide, seasonally resolved temperature fields for the last deglaciation and Holocene.

The various climate forcings have their own seasonal fingerprint. Orbital forcing has a stronger influence on summer temperatures than on winter temperatures, whereas greenhouse gas and AMOC forcings have a stronger impact on winter temperatures. This results in a LGM-to-present temperature difference that is about twice as large in winter as it is in summer. Likewise, the abrupt climate transitions associated with AMOC variations are about 3 times as large in winter temperature as they are in summer temperature. Summer temperatures peak in the early Holocene (10–6 ka BP) following local insolation.

The climate forcings further have a distinct spatial pattern. AMOC-induced climate variations have the largest magnitude in south Greenland and decline toward the north—a pattern that reflects proximity to the North Atlantic. Warming induced by greenhouse gas radiative forcing and insolation forcing typically has the largest magnitude in north Greenland.

Using an ice sheet model, we show that including realistic temperature seasonality has clear implications for the magnitude of simulated LGM GIS volume and the rate and pattern of GIS retreat. Realistic seasonality (1) decreases the size of the simulated LGM ice sheet due to the warmer summers, (2) expedites the onset of deglacial GIS retreat by about 3,000 years, (3) mutes the response to abrupt AMOC-induced climate change, and (4) drives a minimum in GIS volume during the HTM.

Our data-model merged product is a step toward increased realism of deglacial ice sheet model simulations. This will allow for an improved assessment of the GIS sensitivity to climate change during this period of natural climate warming, which can guide future projections of GIS mass loss and attendant sea level rise.

Acknowledgments
We gratefully acknowledge financial support from the U.S. National Science Foundation through grants ARC-1418074 (to A. E. C.), ARC-1417886 (to R. M. D.), ARC-1702920 (to C. B.), and AGS-1502990 (to F. H.); from Geocenter Danmark (to J. E. B.); and from the NOAA Climate and Global Change Postdoctoral Fellowship program, administered by the University Corporation for Atmospheric Research (to F. H. and C. B.). We would like to acknowledge high-performance computing support from Yellowstone (ark:/85065/d7wd3xhc) provided by NCAR's Computational and Information Systems Laboratory, sponsored by the National Science Foundation. This research used resources of the Oak Ridge Leadership Computing Facility at the Oak Ridge National Laboratory, which is supported by the Office of Science of the U.S. Department of Energy under contract DE-AC05-00OR22725. We kindly acknowledge constructive comments by J. Briner and two other anonymous reviewers. The deglacial temperatures are available in the supporting information for selected sites, on the NOAA paleoclimate data center, and from the corresponding author upon request.

References

Abe-Ouchi, A., Segawa, T., & Saito, F. (2007). Climatic conditions for modelling the Northern Hemisphere ice sheets throughout the ice age cycle. *Climate of the Past*, *3*(3), 423–438. https://doi.org/10.5194/cp-3-423-2007

Alley, R. B., & Anandakrishnan, S. (1995). Variations in melt-layer frequency in the GISP2 ice core: Implications for Holocene summer temperatures in central Greenland. *Annals of Glaciology*, *21*(1), 64–70.

Box, J. E. (2013). Greenland ice sheet mass balance reconstruction. Part II: Surface mass balance (1840–2010)*. *Journal of Climate*, *26*(18), 6974–6989. https://doi.org/10.1175/jcli-d-12-00518.1

Bennike, O., & Weidick, A. (2001). Late Quaternary history around Nioghalvfjerdsfjorden and Jøkelbugten, North-East Greenland. *Boreas*, *30*(3), 205–227. https://doi.org/10.1111/j.1502-3885.2001.tb01223.x

Box, J. E., Yang, L., Bromwich, D. H., & Bai, L.-S. (2009). Greenland ice sheet surface air temperature variability: 1840–2007*. *Journal of Climate*, *22*(14), 4029–4049. https://doi.org/10.1175/2009jcli2816.1

Box, J. E., Cressie, N., Bromwich, D. H., Jung, J.-H., van den Broeke, M., van Angelen, J., … Vinther, B. (2013). Greenland ice sheet mass balance reconstruction. Part I: Net snow accumulation (1600–2009). *Journal of Climate*, *26*(11), 3919–3934.

Briner, J. P., Håkansson, L., & Bennike, O. (2013). The deglaciation and neoglaciation of Upernavik Isstrøm, Greenland. *Quaternary Research*, *80*(3), 459–467. https://doi.org/10.1016/j.yqres.2013.09.008

Briner, J. P., Kaufman, D. S., Bennike, O., & Kosnik, M. A. (2014). Amino acid ratios in reworked marine bivalve shells constrain Greenland ice sheet history during the Holocene. *Geology*, *42*(1), 75–78. https://doi.org/10.1130/G34843.1

Briner, J. P., McKay, N. P., Axford, Y., Bennike, O., Bradley, R. S., de Vernal, A., … Wagner, B. (2016). Holocene climate change in Arctic Canada and Greenland. *Quaternary Science Reviews*, *147*, 340–364. https://doi.org/10.1016/j.quascirev.2016.02.010

Briner, J., Stewart, H., Young, N., Philipps, W., & Losee, S. (2010). Using proglacial-threshold lakes to constrain fluctuations of the Jakobshavn Isbræ ice margin, western Greenland, during the Holocene. *Quaternary Science Reviews*, *29*(27), 3861–3874. https://doi.org/10.1016/j.quascirev.2010.09.005

Broecker, W. S. (2006). Abrupt climate change revisited. *Global and Planetary Change*, *54*(3–4), 211–215. https://doi.org/10.1016/j.gloplacha.2006.06.019

Buizert, C., Gkinis, V., Severinghaus, J. P., He, F., Lecavalier, B. S., Kindler, P., … Brook, E. J. (2014). Greenland temperature response to climate forcing during the last deglaciation. *Science*, *345*(6201), 1177–1180. https://doi.org/10.1126/science.1254961

Carlson, A. E., & Clark, P. U. (2012). Ice sheet sources of sea level rise and freshwater discharge during the last deglaciation. *Reviews of Geophysics*, *50*, RG4007. https://doi.org/10.1029/2011RG000371

Carlson, A. E., Winsor, K., Ullman, D. J., Brook, E. J., Rood, D. H., Axford, Y., … Sinclair, G. (2014). Earliest Holocene south Greenland ice sheet retreat within its late Holocene extent. *Geophysical Research Letters*, *41*(15), 5514–5521. https://doi.org/10.1002/2014gl060800

Clark, P. U., Shakun, J. D., Marcott, S. A., Mix, A. C., Eby, M., & Kulp, S. (2016). Consequences of twenty-first-century policy for multi-millennial climate and sea-level change. *Nature Climate Change*, *6*(4), 360–369. https://doi.org/10.1038/nclimate2923

Colville, E. J., Carlson, A. E., Beard, B. L., Hatfield, R. G., Stoner, J. S., Reyes, A. V., & Ullman, D. J. (2011). Sr-Nd-Pb isotope evidence for ice-sheet presence on southern Greenland during the last interglacial. *Science*, *333*(6042), 620–623. https://doi.org/10.1126/science.1204673

Corbett, L. B., Young, N. E., Bierman, P. R., Briner, J. P., Neumann, T. A., Rood, D. H., & Graly, J. A. (2011). Paired bedrock and boulder ^{10}Be concentrations resulting from early holocene ice retreat near Jakobshavn Isfjord, western Greenland. *Quaternary Science Reviews*, *30*(13), 1739–1749. https://doi.org/10.1016/j.quascirev.2011.04.001

Cronauer, S. L., Briner, J. P., Kelley, S. E., Zimmerman, S. R., & Morlighem, M. (2016). ^{10}Be dating reveals early-middle Holocene age of the Drygalski moraines in central west Greenland. *Quaternary Science Reviews*, *147*, 59–68. https://doi.org/10.1016/j.quascirev.2015.08.034

Cuffey, K. M., & Clow, G. D. (1997). Temperature, accumulation, and ice sheet elevation in central Greenland through the last deglacial transition. *Journal of Geophysical Research*, *102*(C12), 26,383–26,396. https://doi.org/10.1029/96JC03981

DeConto, R. M., & Pollard, D. (2016). Contribution of Antarctica to past and future sea-level rise. *Nature*, *531*(7596), 591–597. https://doi.org/10.1038/nature17145

Denton, G. H., Alley, R. B., Comer, G. C., & Broecker, W. S. (2005). The role of seasonality in abrupt climate change. *Quaternary Science Reviews*, *24*(10–11), 1159–1182. https://doi.org/10.1016/j.quascirev.2004.12.002

Dyke, A. S. (2004). An outline of North American deglaciation with emphasis on central and northern Canada. In A. S Dyke (Ed.), *Developments in Quaternary Sciences* (Vol. 2, Part B, pp. 373–424). Amsterdam, Netherlands: Elsevier B.V.

Dyke, L. M., Hughes, A. L., Murray, T., Hiemstra, J. F., Andresen, C. S., & Rodés, Á. (2014). Evidence for the asynchronous retreat of large outlet glaciers in southeast Greenland at the end of the last glaciation. *Quaternary Science Reviews*, *99*, 244–259. https://doi.org/10.1016/j.quascirev.2014.06.001

England, J., Atkinson, N., Bednarski, J., Dyke, A., Hodgson, D., & Cofaigh, C. Ó. (2006). The Innuitian Ice Sheet: Configuration, dynamics and chronology. *Quaternary Science Reviews*, *25*(7), 689–703.

Fluckiger, J., Knutti, R., White, J. W. C., & Renssen, H. (2008). Modeled seasonality of glacial abrupt climate events. *Climate Dynamics*, *31*(6), 633–645. https://doi.org/10.1007/s00382-008-0373-y

Funder, S., Kjaer, K. H., Kjeldsen, K. K., & Cofaigh, C. (2011). The Greenland ice sheet during the past 300,000 years: A review. In J. Ehlers, P. Gibbard, & P. Hughes (Eds.), *Developments in Quaternary Science* (Vol. 15). Amsterdam, Netherlands: Elsevier B.V.

Grootes, P. M., Stuiver, M., White, J. W. C., Johnsen, S., & Jouzel, J. (1993). Comparison of oxygen isotope records from the GISP2 and GRIP greenland ice cores. *Nature*, *366*(6455), 552–554. https://doi.org/10.1038/366552a0

Guillevic, M., Bazin, L., Landais, A., Kindler, P., Orsi, A., Masson-Delmotte, V., … Vinther, B. M. (2013). Spatial gradients of temperature, accumulation and δ^{18}O-ice in Greenland over a series of Dansgaard-Oeschger events. *Climate of the Past*, *9*(3), 1029–1051. https://doi.org/10.5194/cp-9-1029-2013

He, F., Shakun, J. D., Clark, P. U., Carlson, A. E., Liu, Z., Otto-Bliesner, B. L., & Kutzbach, J. E. (2013). Northern Hemisphere forcing of Southern Hemisphere climate during the last deglaciation. *Nature*, *494*(7435), 81–85.

Hughes, A. L., Rainsley, E., Murray, T., Fogwill, C. J., Schnabel, C., & Xu, S. (2012). Rapid response of Helheim Glacier, southeast Greenland, to early Holocene climate warming. *Geology*, *40*(5), 427–430. https://doi.org/10.1130/G32730.1

Intergovernmental Panel on Climate Change (2013). Climate change 2013: The physical science basis. Contribution of Working Group I to the Fifth Assessment Report of the Intergovernmental Panel on, *Climate change* (1535 pp.). New York: Cambridge University Press. https://doi.org/10.1017/CBO9781107415324

Ivanovic, R. F., Gregoire, L. J., Kageyama, M., Roche, D. M., Valdes, P. J., Burke, A., … Tarasov, L. (2016). Transient climate simulations of the deglaciation 21–9 thousand years before present (version 1)—PMIP4 core experiment design and boundary conditions. *Geoscientific Model Development*, *9*(7), 2563–2587. https://doi.org/10.5194/gmd-9-2563-2016

Kelley, S. E., Briner, J. P., & Young, N. E. (2013). Rapid ice retreat in Disko Bugt supported by ^{10}Be dating of the last recession of the western Greenland ice sheet. *Quaternary Science Reviews*, *82*, 13–22. https://doi.org/10.1016/j.quascirev.2013.09.018

Kelly, M. A., Lowell, T. V., Hall, B. L., Schaefer, J. M., Finkel, R. C., Goehring, B. M., … Denton, G. H. (2008). A ^{10}Be chronology of lateglacial and holocene mountain glaciation in the Scoresby Sund region, east Greenland: Implications for seasonality during lateglacial time. *Quaternary Science Reviews*, *27*(25), 2273–2282. https://doi.org/10.1016/j.quascirev.2008.08.004

Kindler, P., Guillevic, M., Baumgartner, M., Schwander, J., Landais, A., & Leuenberger, M. (2014). Temperature reconstruction from 10 to 120 kyr b2k from the NGRIP ice core. *Climate of the Past*, *10*(2), 887–902. https://doi.org/10.5194/cp-10-887-2014

Kobashi, T., Severinghaus, J. P., & Barnola, J. M. (2008). 4 +/- 1.5 degrees C abrupt warming 11,270 yr ago identified from trapped air in Greenland ice. *Earth and Planetary Science Letters*, *268*(3–4), 397–407. https://doi.org/10.1016/j.epsl.2008.01.032

Kobashi, T., Severinghaus, J. P., Brook, E. J., Barnola, J. M., & Grachev, A. M. (2007). Precise timing and characterization of abrupt climate change 8200 years ago from air trapped in polar ice. *Quaternary Science Reviews*, *26*(9–10), 1212–1222. https://doi.org/10.1016/j.quascirev.2007.01.009

Kobashi, T., Kawamura, K., Severinghaus, J. P., Barnola, J.-M., Nakaegawa, T., Vinther, B. M., … Box, J. E. (2011). High variability of greenland surface temperature over the past 4000 years estimated from trapped air in an ice core. *Geophysical Research Letters*, *38*, L21501. https://doi.org/10.1029/2011GL049444

Koerner, R., & Fisher, D. (1990). A record of Holocene summer climate from a Canadian high-arctic ice core. *Nature*, *343*(6259), 630–631.

Landais, A., Caillon, N., Goujon, C., Grachev, A. M., Barnola, J. M., Chappellaz, J., … Leuenberger, M. (2004). Quantification of rapid temperature change during DO event 12 and phasing with methane inferred from air isotopic measurements. *Earth and Planetary Science Letters*, *225*(1-2), 221–232. https://doi.org/10.1016/j.espl.2004.06.009

Larsen, N. K., Funder, S., Kjær, K. H., Kjeldsen, K. K., Knudsen, M. F., & Linge, H. (2014). Rapid early Holocene ice retreat in west Greenland. *Quaternary Science Reviews*, *92*, 310–323. https://doi.org/10.1016/j.quascirev.2013.05.027

Larsen, N. K., Kjær, K. H., Lecavalier, B., Bjørk, A. A., Colding, S., Huybrechts, P., … Olsen, J. (2015). The response of the southern Greenland ice sheet to the Holocene thermal maximum. *Geology*, *43*(4), 291–294. https://doi.org/10.1130/g36476.1

Lecavalier, B. S., Fisher, D. A., Milne, G. A., Vinther, B. M., Tarasov, L., Huybrechts, P., … Dyke A. S. (2017). High arctic Holocene temperature record from the Agassiz ice cap and Greenland ice sheet evolution. *Proceedings of the National Academy of Sciences of the United States of America*, *114*(23), 5952–5957. https://doi.org/10.1073/pnas.1616287114

Lecavalier, B. S., Milne, G. A., Simpson, M. J., Wake, L., Huybrechts, P., Tarasov, L., … Larsen, N. K. (2014). A model of Greenland ice sheet deglaciation constrained by observations of relative sea level and ice extent. *Quaternary Science Reviews*, *102*, 54–84. https://doi.org/10.1016/j.quascirev.2014.07.018

Lecavalier, B. S., Milne, G. A., Vinther, B. M., Fisher, D. A., Dyke, A. S., & Simpson, M. J. (2013). Revised estimates of Greenland ice sheet thinning histories based on ice-core records. *Quaternary Science Reviews*, *63*, 73–82.

Levy, L. B., Kelly, M. A., Lowell, T. V., Hall, B. L., Howley, J. A., & Smith, C. A. (2016). Coeval fluctuations of the Greenland ice sheet and a local glacier, central east Greenland, during late glacial and early Holocene time. *Geophysical Research Letters*, *43*(4), 1623–1631. https://doi.org/10.1002/2015GL067108

Li, C., Battisti, D. S., Schrag, D. P., & Tziperman, E. (2005). Abrupt climate shifts in Greenland due to displacements of the sea ice edge. *Geophysical Research Letters*, *32*, L19702. https://doi.org/10.1029/2005GL023492

Liu, Z., Carlson, A. E., He, F., Brady, E. C., Otto-Bliesner, B. L., Briegleb, B. P., … Zhu, J. (2012). Younger Dryas cooling and the Greenland climate response to CO_2. *Proceedings of the National Academy of Sciences of the United States of America*, *109*(28), 11,101–11,104.

Liu, W., Liu, Z., Cheng, J., & Hu, H. (2015). On the stability of the Atlantic Meridional Overturning Circulation during the last deglaciation. *Climate Dynamics*, *44*(5–6), 1257. https://doi.org/10.1007/s00382-014-2153-1

Liu, Z., Otto-Bliesner, B. L., He, F., Brady, E. C., Tomas, R., Clark, P. U., … Cheng, J. (2009). Transient simulation of last deglaciation with a new mechanism for Bølling-Allerød warming. *Science*, *325*(5938), 310–314. https://doi.org/10.1126/science.1171041

Marcott, S. A., Bauska, T. K., Buizert, C., Steig, E. J., Rosen, J. L., Cuffey, K. M., … Brook, E. J. (2014). Centennial-scale changes in the global carbon cycle during the last deglaciation. *Nature*, *514*, 616–619. https://doi.org/10.1038/nature13799

Marcott, S. A., Shakun, J. D., Clark, P. U., & Mix, A. C. (2013). A reconstruction of regional and global temperature for the past 11,300 years. *Science*, *339*(6124), 1198–1201. https://doi.org/10.1126/science.1228026

Martin, M. A., Winkelmann, R., Haseloff, M., Albrecht, T., Bueler, E., Khroulev, C., & Levermann, A. (2011). The Potsdam Parallel Ice Sheet Model (PISM-PIK)—Part 2: Dynamic equilibrium simulation of the Antarctic ice sheet. *The Cryosphere*, *5*(3), 727–740. https://doi.org/10.5194/tc-5-727-2011

McManus, J. F., Francois, R., Gherardi, J. M., Keigwin, L. D., & Brown-Leger, S. (2004). Collapse and rapid resumption of Atlantic meridional circulation linked to deglacial climate changes. *Nature*, *428*(6985), 834–837. https://doi.org/10.1038/nature02494

Menviel, L., Timmermann, A., Timm, O. E., & Mouchet, A. (2011). Deconstructing the last glacial termination: The role of millennial and orbital-scale forcings. *Quaternary Science Reviews*, *30*(9–10), 1155–1172. https://doi.org/10.1016/j.quascirev.2011.02.005

Mitchell, J. F. B. (1989). The effect and climate change. *Reviews of Geophysics*, *27*(1), 115–139. https://doi.org/10.1029/RG027i001p00115

Monnin, E., Indermühle, A., Dällenbach, A., Flückiger, J., Stauffer, B., Stocker, T. F., … Barnola, J.-M. (2001). Atmospheric CO_2 concentrations over the last glacial termination. *Science*, *291*(5501), 112–114.

NEEM community members (2013). Eemian interglacial reconstructed from a Greenland folded ice core. *Nature*, *493*(7433), 489–494.
NGRIP community members (2004). High-resolution record of Northern Hemisphere climate extending into the last interglacial period. *Nature*, *431*(7005), 147–151. https://doi.org/10.1038/nature02805
Pausata, F. S., & Löfverström, M. (2015). On the enigmatic similarity in Greenland δ^{18}O between the Oldest and Younger Dryas. *Geophysical Research Letters*, *42*(23), 10,470–10,477. https://doi.org/10.1002/2015gl066042
Peltier, W. (2004). Global glacial isostasy and the surface of the ice-age Earth: The ICE-5G (VM2) model and GRACE. *Annual Review of Earth and Planetary Sciences*, *32*, 111–149.
Pollard, D., & DeConto, R. M. (2012). Description of a hybrid ice sheet-shelf model, and application to Antarctica. *Geoscientific Model Development*, *5*(5), 1273–1295. https://doi.org/10.5194/gmd-5-1273-2012
Pollard, D., DeConto, R. M., & Alley, R. B. (2015). Potential Antarctic ice sheet retreat driven by hydrofracturing and ice cliff failure. *Earth and Planetary Science Letters*, *412*, 112–121. https://doi.org/10.1016/j.epsl.2014.12.035
Rinterknecht, V., Jomelli, V., Brunstein, D., Favier, V., Masson-Delmotte, V., Bourlès, D., … Leanni, L. (2014). Unstable ice stream in Greenland during the Younger Dryas cold event. *Geology*, *42*(9), 759–762. https://doi.org/10.1130/G35929.1
Ritz, C., Rommelaere, V., & Dumas, C. (2001). Modeling the evolution of Antarctic ice sheet over the last 420,000 years: Implications for altitude changes in the Vostok region. *Journal of Geophysical Research*, *106*(D23), 31,943–31,964. https://doi.org/10.1029/2001JD900232
Robinson, A., Calov, R., & Ganopolski, A. (2012). Multistability and critical thresholds of the Greenland ice sheet. *Nature Climate Change*, *2*(6), 429–432. https://doi.org/doi:10.1038/nclimate1449
Schaefer, J. M., Finkel, R. C., Balco, G., Alley, R. B., Caffee, M. W., Briner, J. P., … Schwartz, R. (2016). Greenland was nearly ice-free for extended periods during the Pleistocene. *Nature*, *540*(7632), 252–255. https://doi.org/10.1038/nature20146
Seierstad, I., Abbott, P., Bigler, M., Blunier, T., Bourne, A., Brook, E., … Vinther, B. (2014). Consistently dated records from the greenland GRIP, GISP2 and NGRIP ice cores for the past 104 ka reveal regional millennial-scale isotope gradients with possible Heinrich event imprint. *Quaternary Science Reviews*, *106*, 29–46. https://doi.org/10.1016/j.quascirev.2014.10.032
Severinghaus, J. P., Sowers, T., Brook, E. J., Alley, R. B., & Bender, M. L. (1998). Timing of abrupt climate change at the end of the Younger Dryas interval from thermally fractionated gases in polar ice. *Nature*, *391*(6663), 141–146.
Simon, K., James, T., & Dyke, A. (2015). A new glacial isostatic adjustment model of the Innuitian Ice Sheet, arctic Canada. *Quaternary Science Reviews*, *119*, 11–21. https://doi.org/https://doi.org/10.1016/j.quascirev.2015.04.007
Simpson, M. J. R., Milne, G. A., Huybrechts, P., & Long, A. J. (2009). Calibrating a glaciological model of the Greenland ice sheet from the Last Glacial Maximum to present-day using field observations of relative sea level and ice extent. *Quaternary Science Reviews*, *28*(17–18), 1631–1657. https://doi.org/10.1016/j.quascirev.2009.03.004
Sinclair, G., Carlson, A., Mix, A., Lecavalier, B., Milne, G., Mathias, A., … DeConto, R. (2016). Diachronous retreat of the Greenland ice sheet during the last deglaciation. *Quaternary Science Reviews*, *145*, 243–258. https://doi.org/10.1016/j.quascirev.2016.05.040
Talley, L. D. (2013). Closure of the global overturning circulation through the Indian, Pacific, and Southern oceans: Schematics and transports. *Oceanography*, *26*, 80–97.
Tarasov, L., & Richard Peltier, W. (2002). Greenland glacial history and local geodynamic consequences. *Geophysical Journal International*, *150*(1), 198–229.
Ullman, D. J., Carlson, A. E., Hostetler, S. W., Clark, P. U., Cuzzone, J., Milne, G. A., … Caffee, M. (2016). Final Laurentide ice-sheet deglaciation and Holocene climate-sea level change. *Quaternary Science Reviews*, *152*, 49–59. https://doi.org/10.1016/j.quascirev.2016.09.014
Van den Broeke, M., Bamber, J., Ettema, J., Rignot, E., Schrama, E., van de Berg, W. J., … Wouters, B. (2009). Partitioning recent Greenland mass loss. *Science*, *326*(5955), 984–986. https://doi.org/10.1126/science.1178176
Vinther, B. M., Buchardt, S. L., Clausen, H. B., Dahl-Jensen, D., Johnsen, S. J., Fisher, D. A., … Svensson, A. M. (2009). Holocene thinning of the Greenland ice sheet. *Nature*, *461*(7262), 385–388.
Winsor, K., Carlson, A. E., Caffee, M. W., & Rood, D. H. (2015). Rapid last-deglacial thinning and retreat of the marine-terminating southwestern Greenland ice sheet. *Earth and Planetary Science Letters*, *426*, 1–12. https://doi.org/10.1016/j.epsl.2015.05.040
Winsor, K., Carlson, A. E., Welke, B. M., & Reilly, B. (2015). Early deglacial onset of southwestern Greenland ice-sheet retreat on the continental shelf. *Quaternary Science Reviews*, *128*, 117–126. https://doi.org/10.1016/j.quascirev.2015.10.008
Yau, A. M., Bender, M. L., Robinson, A., & Brook, E. J. (2016). Reconstructing the last interglacial at Summit, Greenland: Insights from GISP2. *Proceedings of the National Academy of Sciences of the United States of America*, *113*(35), 9710–9715. https://doi.org/10.1073/pnas.1524766113
Young, N. E., & Briner, J. P. (2015). Holocene evolution of the western Greenland ice sheet: Assessing geophysical ice-sheet models with geological reconstructions of ice-margin change. *Quaternary Science Reviews*, *114*, 1–17. https://doi.org/10.1016/j.quascirev.2015.01.018
Young, N. E., Briner, J. P., Axford, Y., Csatho, B., Babonis, G. S., Rood, D. H., & Finkel, R. C. (2011). Response of a marine-terminating Greenland outlet glacier to abrupt cooling 8200 and 9300 years ago. *Geophysical Research Letters*, *38*, L24701. https://doi.org/10.1029/2011GL049639
Young, N. E., Briner, J. P., Rood, D. H., Finkel, R. C., Corbett, L. B., & Bierman, P. R. (2013). Age of the Fjord Stade moraines in the Disko Bugt region, western Greenland, and the 9.3 and 8.2 ka cooling events. *Quaternary Science Reviews*, *60*, 76–90. https://doi.org/10.1016/j.quascirev.2012.09.028
Young, N. E., Briner, J. P., Stewart, H. A., Axford, Y., Csatho, B., Rood, D. H., & Finkel, R. C. (2011). Response of Jakobshavn Isbræ, Greenland, to Holocene climate change. *Geology*, *39*(2), 131–134. https://doi.org/10.1130/G31399.1
Zreda, M., England, J., Phillips, F., Elmore, D., & Sharma, P. (1999). Unblocking of the Nares Strait by Greenland and Ellesmere ice-sheet retreat 10,000 years ago. *Nature*, *398*(6723), 139–142.